iJRASET
International Journal For Research in Applied Science and Engineering Technology

INTERNATIONAL JOURNAL FOR RESEARCH

IN APPLIED SCIENCE & ENGINEERING TECHNOLOGY

Volume: 9 **Issue:** IX **Month of publication:** September 2021

DOI: https://doi.org/10.22214/ijraset.2021.38024

www.ijraset.com

Call: 08813907089 | E-mail ID: ijraset@gmail.com

International Journal for Research in Applied Science & Engineering Technology (IJRASET)
ISSN: 2321-9653; IC Value: 45.98; SJ Impact Factor: 7.429
Volume 9 Issue IX Sep 2021- Available at www.ijraset.com

Thermal Analysis of Microchannels Heat Sink using Super-hydrophobic Surface

Shubham Jawade[1], Prof. S. M. Lawankar[2]
[1] *PG Student,* [2]*Prof. Dept. of Mechanical Engineering Govt. College of Engineering Amravati, India*

Abstract: ***Electronics devices are the major part of modern technology and with the rapid growth of miniaturizations of electronic devices, the heat dissipation from these devices have been the objective for researchers. This heat dissipation has to done effectively otherwise this will affect the life of device and will result decrement in efficiency. Increasing the heat transfer rates from electronic devices has long been a quest. Microchannel heat sink is one of the best option for removing heat from the electronics devices due to its compact size which provides high surface area to volume ratio that enables higher heat transfer rates. Microchannels are the flow passages having hydraulic diameter ranges from 10 micrometer (µm) to 200µm. Microchannel heat sink enhances the feasibility of electronics device. Microchannels with hydrophobic surface are a promising candidate for cooling of electronics devices, as hydrophobic surface can be used to create friction free regions with a channel which effectively reduce pumping power, flow pressure drop and frictional factor compared to Microchannel without Hydrophobic surface. This paper deals with the detailed behavior of Microchannel with hydrophobic surface. In this work, rectangular cross section with 0.8 mm (800 micron) hydraulic diameter super hydrophobic microchannel is used.***

Keywords: Microchannel, Hydrophobic surface, Heat transfer rate, Frictional factor.

I. INTRODUCTION

Heat exchangers are a core component to almost every modern energy system from microscale electronic packaging to city-scale power plants design, thermal energy management is everywhere. Transfer of heat from one place to another, from one medium to another, and meeting the challenges and bring out the result under a various condition have been the objective. Heat transfer by convection transfers the heat quickly away from heat exchanger.

The equation of heat transfer by convection is:

$q = hA (T_s - T_f)$

h = Heat Transfer Coefficient (W/m^2K)

A = Surface Area (m^2)

T_s = Surface Temperature (K)

T_f = Fluid Temperature (K)

The early development focused on increasing the surface area to get higher heat transfer rates.

Later on the era of compact heat exchanger began and researcher revisited the equation, this time the importance is given to improving h & A simultaneously.

Nature provides us with some important clues regarding the heat and mass transfer processes. Looking at the human body the blood vessel that are largely responsible for thermal exchange have diameter about 175µm. From human body we understand that with smaller diameter we are getting higher heat transfer rates. The heat transfer coefficient equation is given as $h=N_u k/D_h$.

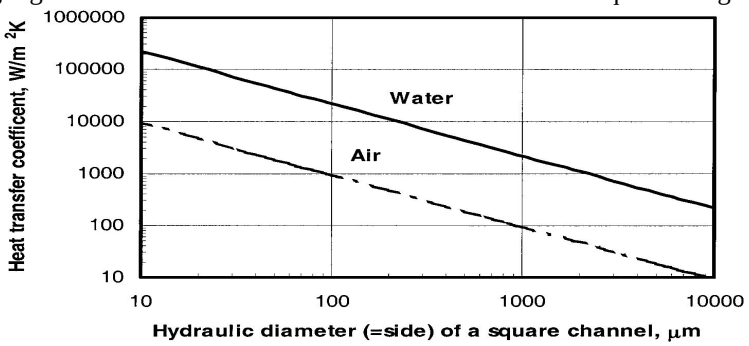

Fig. 1 Variation of heat transfer coefficient with channel size for a square channel

As the heat transfer coefficient is inversely proportional to hydraulic diameter (D_h) with decrease in hydraulic diameter the heat transfer coefficient will increase so as the Heat Transfer rate. The effect of Hydraulic diameter on heat transfer coefficient is shown in Fig. 1 for water and air flowing in rectangular channel under constant heat flux. Fig. 1 shows the variation of h with channel hydraulic diameter. The prominent enhancement in *h* with a reduction in channel size is clearly demonstrated. The rapidly increasing demand for micro-electronic systems provides a significant in a high amount of heat dissipation and thermal control. Numerous techniques are being developed to keep the device temperature under the critical limit where high heat flux is generated. Microchannels heat sinks are compact and innovative temperature reduction technology for the removal of a large amount of heat from a small area. Microchannels are microscale fluid passages which have a hydraulic diameter in the range of 10µm to 200µm. The small passages provide the high surface area to volume ratio that increases heat transfer rates. The compactness and high heat transfer carrying capacity of microchannels heat sinks make them very effective differentiating them from conventional heat sink.

Since heat transfer enhancements are usually associated with increases in pumping power due to increased flow friction (for surface force dominant microchannels) or increased viscoelastic frictional drag (for nanofluids), there exists a need to reduce the flow friction in both of these technologies (microchannels and nanofluids). One approach that shows potential to reduce friction is the use of hydrophobic surfaces. Inspired by the lotus leaf, hydrophobic surfaces are consisting of engineered microstructures includes square posts and holes, transverse and longitudinal grooves which reduce the surface energy and result in nearly perfect hydrophobicity.

II. LITERATURE REVIEW

Tuckerman and Pease [1] They introduced the first microchannel in 1981. They designed a rectangular microchannel heat sink in a 1*1 cm² silicon wafer. The dimensions of the rectangular wafer were 50µm width and 302µm depth and it was separated by 50µm thick walls. They have demonstrated that the electronic chip can be effectively cooled by means of water flow in microchannels fabricated on the circuit board on which the chips are mounted. The microchannel was able to dissipate around 790 W/cm² with a maximum substrate temperature rise of 71ºC above water inlet temperature and a 2.2 bar pressure drop.

Sasaki and Kishimoto [2] They reported that for increasing cooling capability with a constant rate of coolant flow it is desirable to reduce the channels width below 100µm but at the same time pressure drop is also increase. With the reduction of channel cross-section, the pressure drop is increasing. When channel width is 50µm and the outside dimension of the silicon chip is 10mm square, the pressure drop became 20000kg/m^2. After performing the experiments, they have obtained an optimized channel width for maximum heat transfer by the microchannel.

B.X. Wang et al. [3] They tested 6 kinds of microchannels (stainless steel plates) structure, each microchannel cross section was rectangular with different width and identical channel height of 700µm. Methanol and deionized water were employed as the working fluid. For single phase liquid forced convection through microchannels, a fully developed heat transfer regime is initiated at about Reynolds Number = 1000 – 1500. They also reported that transition and laminar heat transfer in microchannels are highly strange and complicated, compared with conventional size situation. The range of transition zone and heat transfer characteristics of both transition and laminar flow are highly affected by liquid temperature, velocity and microchannel size.

Peng and Peterson [4] The forced convective heat transfer and flow characteristics of water flowing through microchannel plates with extremely small rectangular channels having hydraulic diameters of 0.133 - 0.367 mm and different geometric configurations were investigated experimentally. Laminar heat transfer does depend on parameters D_h/W_c (D_h=Hydraulic diameter, W_c = Centre to centre distance of Microchannels) and H/W_c (H=Height of Microchannel, W=Width of Microchannel) while turbulent convection is related to D_h/W and Z (Z= Dimensional ratio) and it was found that the dimensionless ratio, Z = 0.5, is the optimum configuration for turbulent heat transfer. Investigated frictional factor of liquid flow in the microstructures experimentally and analytically. Their experiments demonstrated the importance of the geometric parameters, including the hydraulic diameter, H/W or Z, and D_h/W_c, on the friction factor. The laminar friction factor or flow resistance reaches a minimum value as Z approaches 0.5.

Yoichi Murakami et al. [5] Reported the effect of Ratio of channels area to heat sink area on minimum dimensional pumping power and minimum dimensional pressure drop. Minimum dimensional pumping power and minimum dimensional pressure drop always decreases with the increase in ratio of channel area to heat sink area. Suggest the optimum ratio of channel area to heat sink area which is 0.3, where the chip size is 15mm×15mm×0.3mm, ΔT (Maximum Temperature Difference) is 50ºC and maximum Heat transfer is 400W with volumetric flow rate of 2.90 cm^3/s and Pumping power of 0.213W.

Satish Kandlikar et al. [6] suggested the criteria for classification of the channels based on the range of hydraulic diameter (D_h). Minichannel: 3mm ≥ D_h ≥ 200µm, Microchannel: 200µm ≥ D_h ≥10µm. Reported the effect of hydraulic diameter on heat transfer coefficient and pressure gradient, with the reduction of hydraulic diameter the heat transfer coefficient and pressure gradient increasing rapidly. Also suggest the Knudsen number ranges for type of flow, and introduces to microfabrication technology.

H. Y. Zhang et al. [7] The heat sink was fabricated by micro end milling microchannels on an aluminium block of 50 mm (L) × 24 mm × (W) 2.8 mm (H) with natural finish and then anodized to protect against corrosion. It had 21 channels and a finned area of 15 mm (L) × 12.2 mm (W), each channel being 0.21 mm wide and 2 mm high. The large aspect ratio of 9.5 has been purposely made to enlarge the surface area for heat transfer. De-ionized water was used as the coolant, Taking the maximum flow rate of 1.67×10^{-5} m^3/s, the thermal resistance is found to be 0.317 ºC/W and thus the maximum power dissipation of 189 W or 131 W/cm2 is expected with a temperature difference of 60 ºC between the component and the inlet fluid.

Poh-Seng Lee et al. [8] Studied heat transfer in microchannels of different sizes (with hydraulic diameters of 318–903 μm) was experimentally investigated over a range of flow rates. Consider Single-phase flows in the thermally developing laminar regimes and found out heat transfer coefficient increased with decreasing channel size at a given flow rate. Carried out numerical simulations for developing flows in rectangular channels based on a conventional Navier-Stokes' analysis, using both a full 3D conjugate approach and a simplified thin wall model. Numerical results and experimental data were found to be in good agreement and results also confirm that the simplified thin wall analysis can be used as a computationally economical alternative to a full 3D conjugate analysis.

Jie Jiang et al. [9] used deionized water as the working fluid and the flow and heat transfer characteristics in rectangular microchannels were tested. With increase in Reynolds number the friction factor in microchannels decreases and the value is smaller than that in the conventional condition, which is only 20–30% of the conventional value in the present study. The critical Reynolds number is smaller than the conventional one and is about 1100. The Nusselt number almost remains constant in the laminar flow and is smaller than that for the convectional channel. They found out the effect of heat flux on the Nusselt number, with small flow rate the Nusselt number remains a constant and with the larger flow rate Nusselt number increases with the increase in the heat flux.

Shou-Shing Hsieh et al. [10] Liquid microchannel fluid flow and heat transfer with one-sided heating (both isothermal and isoflux) was studied for four different test fluids (deionized water, methanol, 50 wt% DI water/50 wt% methanol mixture, and ethanol solution) at $5 \leq Re \leq 240$ and the corresponding $20 \leq Pe \leq 2300$ with hydrophobic and hydrophilic surface property through μPIV for velocity and μLIF for temperature measurements.

Yongpan Cheng et al. [11] Microchannels with superhydrophobic surfaces are a promising candidate for electric cooling with mild frictional penalty. Frictional and thermal performance of laminar liquid-water flow in such microchannels is numerically investigated for various shear-free fractions and Reynolds numbers. The structures on superhydrophobic surfaces include square posts and holes, transverse and longitudinal grooves. Combined frictional and thermal performance of microchannels is evaluated by a goodness factor, and is compared with that of smooth plain channels. It is found that with increasing shear-free fractions, both friction factor and average Nusselt number deteriorate for four surface patterns; however, goodness factor is improved significantly over smooth plain channels.

Jing ZHOU et al. [12] Experimented on 3 Ton residential heat pump system, Tube and fin heat exchanger (TFHE) and Microchannel heat exchanger (MCHE) were compared and using MCHE the cooling rate can increase by 4%, SEER and HSPF can increase by 2% and 1%, weight of the heat exchanger can be reduced by 44% and the refrigerant charge can be reduced by 51%. For the 65kW commercial heat pump system, the cooling capacity can increase by 2% by using MCHE, and EER can increase by 4%. The weight of heat exchangers can be reduced by 35%. And the refrigerant charge can be reduced by 40% and concluded that MCHE has higher heat transfer performance, much lower weight and refrigerant charge, which is a good choice for improving the efficiency and saving cost.

Ali Heidarian et al. [13] Nanofluids and hydrophobic and superhydrophobic walls for microchannels heat sinks has been studied. Two types of nanofluids were used (water/Al_2O_3 and water/TiO_3). Applying the hydrophobic and superhydrophobic surface caused non zero velocity over the walls and reduce the wall shear stress. Microchannels with hydrophobic walls required 12% less pumping power than those with hydrophilic walls. The superhydrophobic wall caused a 66% reduction in the required pumping power. With increasing the Reynolds number, pressure drop and the Nusselt number increased, and better thermal performance was obtained.

M. Spizzichino et al. [14] The thermo-hydrodynamic behaviour of a square cross-section standard serpentine cell and a new wavy-sinusoidal serpentine cell were investigated and compared with a classical straight parallel channel configuration, to be considered as reference. Tested the heat transfer properties and the detailed fluid flow behaviours and found out range of Reynolds number in the regime from 50 to 1500, up to the turbulent regime with Reynolds number as large as 4000. Nusselt number and Reynolds number have increase and frictional factor has reduced in case of standard serpentine and wavy serpentine compared to straight parallel channels, which reduce the pressure drop, pumping power and increase heat transfer rate.

ISSN: 2321-9653; IC Value: 45.98; SJ Impact Factor: 7.429
Volume 9 Issue IX Sep 2021- Available at www.ijraset.com

III. EXPERIMENTAL PROCEDURES

This chapter is devoted to a thorough presentation of all the aspects of the procedure followed in designing and manufacturing of the microchannel and constructing the experimental setup, including preliminary stages and various difficulties encountered. The experimental data are given concisely at the end of the chapter.

A. Design of Microchannels

The first step of the work leading to a set of experimental results on the thermal performance of a microchannel was to investigate the manufacturing methods suitable for the geometry. Micromachining is more suitable for the geometry as it offers high accuracy for the channel depth. The second step of the work is to find material for microchannel would preferably with high thermal conductivity, such as aluminium or copper.

B. Manufacturing of Microchannels

Aluminium is preferred as the material for microchannel heat sink because of its high thermal conductivity. Fig. 2 shows the three-dimensional view of a microchannel heat sink with 17 channels using Unigraphics modelling package.

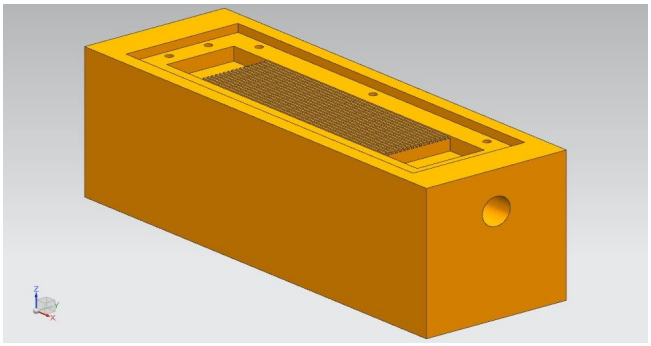

Fig 2- 3D model of microchannels

The fabricated HSS flat type milling cutter is mounted on the Arbor of the universal milling machine. Aluminium block of length 150 mm, width 50 mm and height 50 mm are used for making microchannel heat sink. The respective block is held on the machine vice mounted on the table of the milling machine to machine the required numbers of channels. The rectangular microchannels of 800µm width and 800µm microns depth are machined in the aluminium block to form the microchannel heat sink. Thus, heat sink with 17 numbers of microchannels are fabricated using the aluminium block. Soluble oil is used as coolant during machining in order to obtain good surface finish.

Hydrophobic layer is applied on the microchannels in two-step process, aluminium substrates were initially cleaned with acetone and distilled water multiple times, then aluminium substrates were immersed in a mixture of 10 gm/litre KOH in distilled water solution for 5–60 min. KOH solution roughed the aluminium surfaces as shown in Figure. Subsequently, aluminium substrates were rinsed with distilled water and ethanol. Finally, they were immersed in 20 gm/litre ethanol solution of lauric acid for 30 min and then they were dried in air for 20 hour. Lauric acid here lowered the surface energy of aluminium surface.

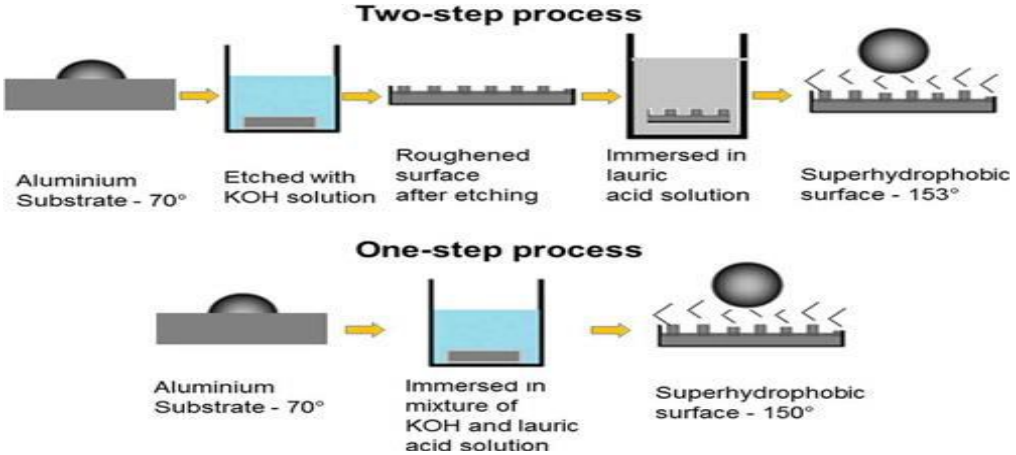

Fig. 3 steps to apply hydrobhopic layer

C. Experimental Setup

The Syringe pump is connected to the inlet port of the microchannel. The outlet port of the outlet plenum is connected to the collecting tank. The mass flow rate of the coolant is varied by adjusting the flow control knob in the pump. Figure shows the diagram of experimental setup.

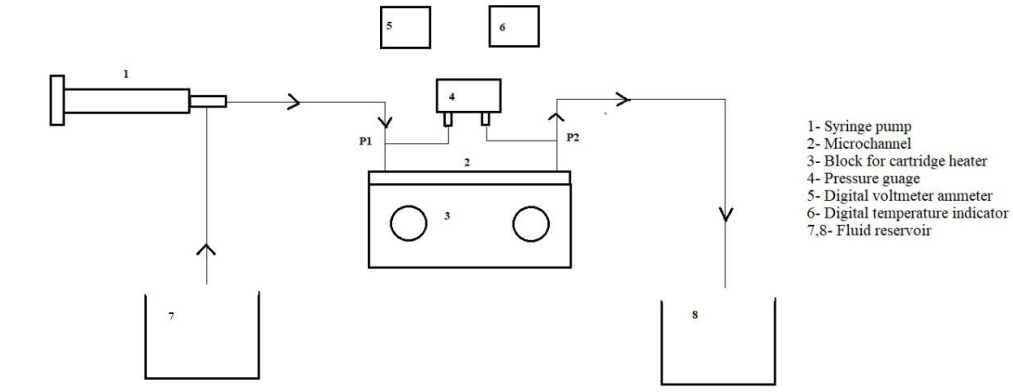

Fig.4 Line diagram of experimental setup

Fig. 5 Microchannel assembly

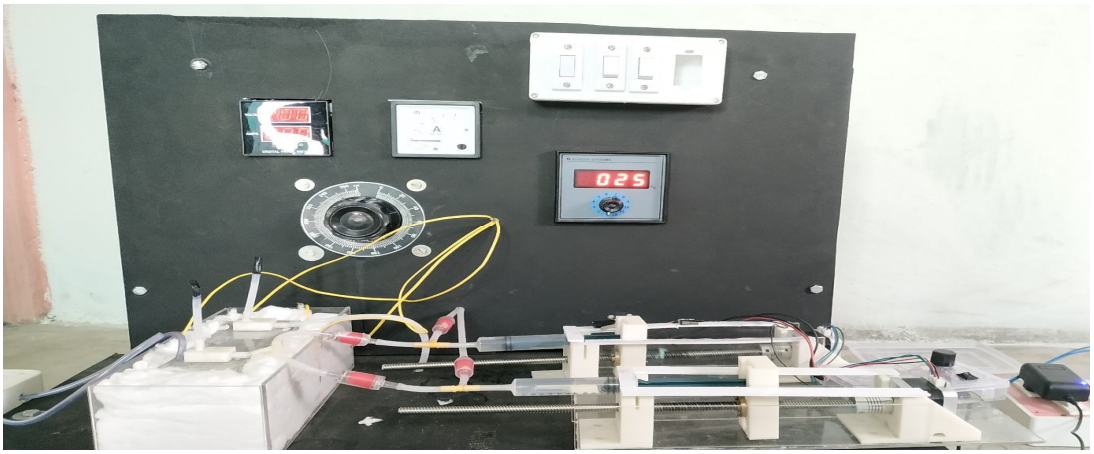

Fig. 6 Actual test setup

Experiments have been conducted using different mass flow rate of water by varying heat input. The water inlet temperature, water outlet temperature, wall temperature and pressure drop is measured.

D. Experiment

The changeable and manageable variables of the test setup were selected as flow rates of water. The flow rates of water were adjusted by changing pump input voltage. The flow rates of water were selected as 0.0006667 kg/s, 0.0005 kg/s and 0.0004167 kg/s. All experimental input parameters are listed in Table. The heat input changed from 60 W to 100 W. The observation table is for mass flow rate of 0.0006667 kg/s, 0.0005 kg/s and 0.0004167 kg/s with different heat input as 60 W, 80W and 100W.

Table I Observation table

Sr. No	$\dot{m}_t$ (kg/s)	Q (W)	T_{in}(°C)	T_{out}(°C)	T_w(°C)	ΔP(Pa)
1	0.0006667	60	25	45.66667	48.16667	330
2	0.0006667	80	23	50.5	55.16667	330
3	0.0006667	100	25	59.66667	65.58333	330
	0.0005	60	25	50.16667	55.33333	290
5	0.0005	80	24	58.66667	63.75	290
6	0.0005	100	24	68.66667	74	290
7	0.0004167	60	26	55.5	59.16667	260
8	0.0004167	80	25	64.66667	70.08333	260
9	0.0004167	100	26	78.16667	83.33333	260

IV. EXPERIMENTAL RESULT

The heat removed by water can be calculated by knowing the total mass flow rate, specific heat of water and the difference in temperatures. The heat removed by water is found out using the Equation

$Q_w = m_t * C_p * \Delta T$

For given heat input and mass flow rate, the rate of heat removed by water for various number of microchannels are presented in Table. It is concluded that heat removed by the water increases with heat supplied, due to higher temperature difference between inlet water and microchannel heat sink temperature. The heat removed by the water increases with mass flow rate for given heat input, since the heat transfer rate increases as mass flow rate of water increases.

A. Effect of Reynold number on Pressure drop

Fig. 7 shows pressure drop increases with increase in Reynold number this because of the reduction in friction factor with Reynold number. An increase of Reynold number, reflecting an increase of the water flow intensity, resulted in an increased flow resistance. Maximum value of pressure drop found to be 330 Pa at 78.22253 Reynold number.

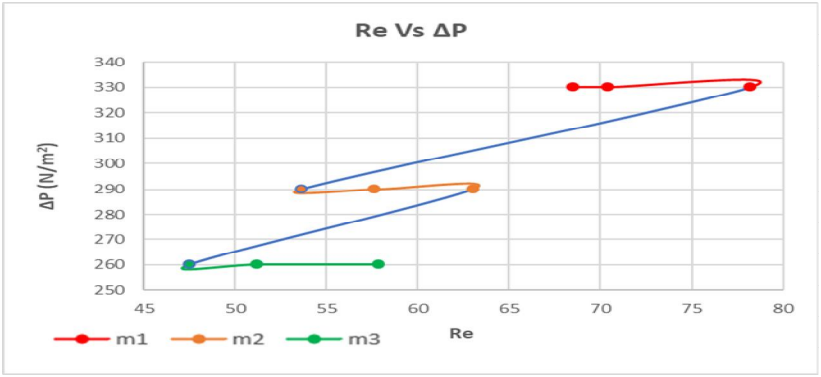

Fig. 7 Reynold number (Re) Vs pressure drop (ΔP)

Fig. 7 represents the graph between Reynolds's number and pressure difference. As it can be seen that, for different mass flow rates different pressure difference is occur. The maximum pressure difference occurs at a mass flow rate of 0.0006667 kg/s is 330 Pa. The minimum pressure difference occurs at the mass flow rate of 0.0004167 kg/s is 260 Pa. It can also be seen that for the mass flow rate 0.0006667 kg/s, the pressure difference increases drastically after Reynolds number 72.22253. From the above Fig. 7 it can conclude that higher the mass flow rate higher the Reynolds number and higher the pressure difference.

B. Effect of Reynolds number on Friction factor

Fig. 8 shows friction factor reduces with increase in Reynold number This is because, when Re increases, the velocity gradient also increases but at a lesser rate. For all the cases of water flow in microchannels, similarly, a linear drop of the value of frictional factor has been observed in the laminar flow.

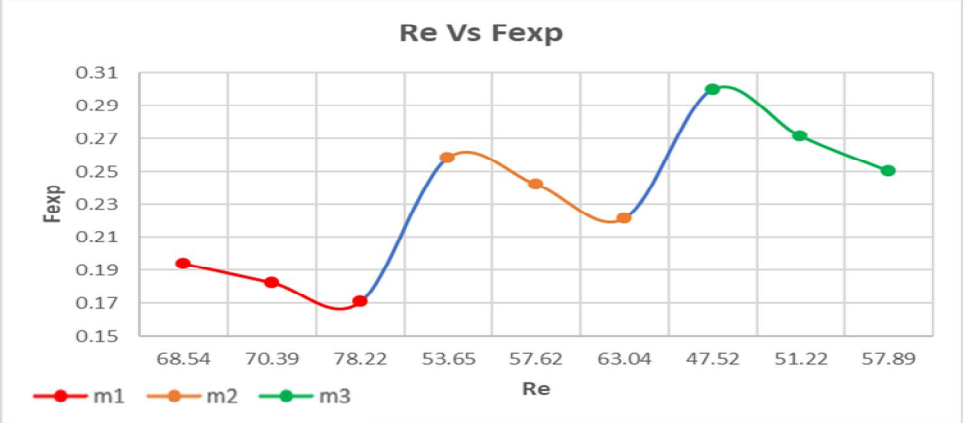

Fig. 8 Reynold number Vs Experimental Friction factor

Fig. 8 represents the graph between Reynolds's number and experimental friction factor. The above graph is plotted for the mass flow rate of 0.0006667 kg/s, 0.0005 kg/s and 0.0004167 kg/s. From the Figure it can see that as Reynolds number of the system is increases the friction factor is decreases. The maximum friction factor occurs at a Reynolds number of 47.51473 is 0.299703 while minimum friction factor occurs at a Reynolds number of 78.22253 is 0.170875. Hence it can conclude that Experimental friction factor is inversely proportion to the Reynolds number.

C. Effect of pressure drop on heat transfer coefficient

Fig. 9 shows heat transfer coefficient increases with increase in pressure drop. This is because of decrease in friction factor in case of hydrophobic microchannels. Friction increases the pressure at outlet and hence decreases the pressure drop.

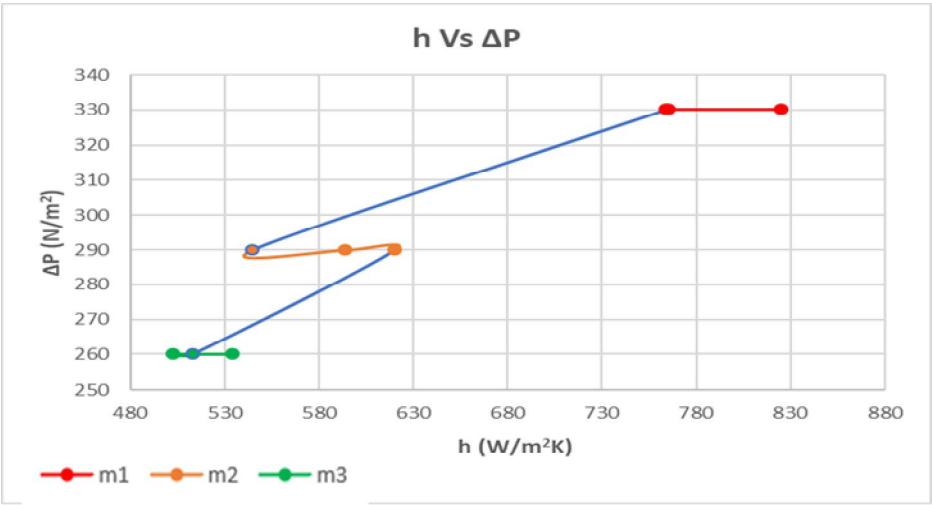

Fig. 9 Heat transfer coefficient (h) Vs Pressure drop (ΔP)

Figure represents the graph between pressure drop and convective heat transfer coefficient. The above graph is plotted for the mass flow rate of 0.0006667 kg/s, 0.0005 kg/s and 0.0004167 kg/s. From the Figure it can see that as pressure drop of the system is increases the convective heat transfer coefficient is also increases. The maximum convective heat transfer coefficient occurs at a pressure drop of 330 Pa is 825.5501 W/m^2K while minimum convective heat transfer coefficient occurs at a pressure drop of 260 Pa is 503.2014 W/m^2K. Hence it can conclude that pressure drop has exponential relationship with convective heat transfer coefficient.

D. Effect of Heat Flux on Temperature Difference at Different Mass Flow Rate

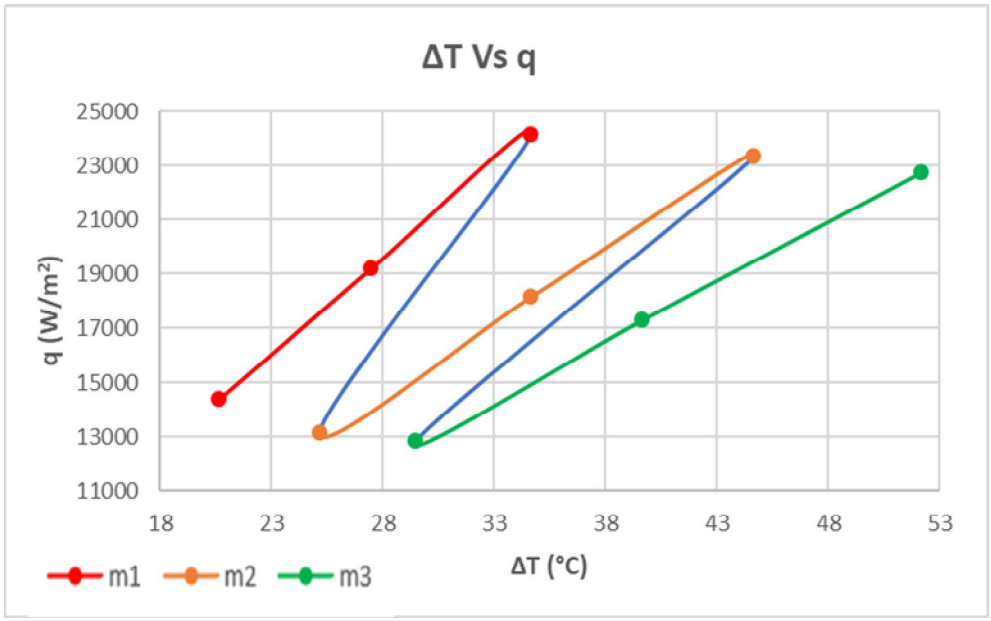

Fig. 10 Temperature difference(ΔT) Vs heat flux (q)

Fig. 10 represents the graph between heat flux and temperature difference. As it can be seen that, for different mass flow rates different temperature difference is occur. The maximum heat flux occurs at a temperature difference of 34.66667 (°C) is 24163.88 W/m^2 at a mass flow rate of 0.0006667 kg/s. The minimum heat flux occurs at a temperature difference of 29.5 (°C) is 12851.04 W/m^2 at a mass flow rate of 0.0004167 kg/s. From the above Figure it can conclude that higher the mass flow rate higher the heat flux.

E. Comparison of Theoretical and Experimental Friction Factor

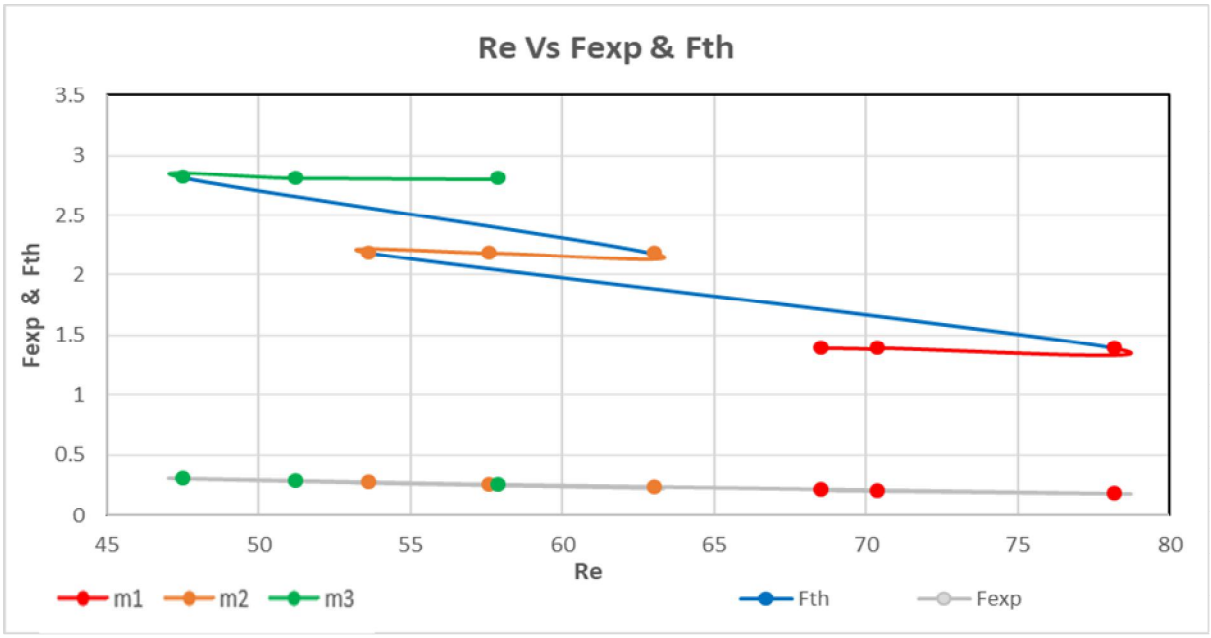

Fig. 11 Reynold number (Re) Vs Experimental friction (Fexp) and theoretical friction (Fth)

Fig. 11 shows comparison of friction factor between theoretical and experimental. Experimental friction factor much lesser than theoretical this is because of hydrophobic layer on channel during experimentation.

V. NUMERICAL MODELING

The present work investigates the effect of wide range of parameters to the heat transfer from microchannel. The three-dimensional governing equations representing fluid flow, heat transfer is solved using finite volume based computational fluid dynamics (CFD) code, FLUENT.

A. Governing Equation

The natural convection flow under investigation was modelled by a set of partial differential equations describing the conservation of mass, momentum and energy in three-dimensional Cartesian coordinate system.

Conservation of mass

$$\frac{\partial(\rho u)}{\partial x} + \frac{\partial(\rho v)}{\partial y} + \frac{\partial(\rho w)}{\partial z} = 0$$

Conservation of momentum

$$\frac{\partial(\rho u^2)}{\partial x} + \frac{\partial(\rho uv)}{\partial y} + \frac{\partial(\rho uw)}{\partial z} = -\frac{\partial(p_0)}{\partial x} + \rho\nu\left(\frac{\partial^2 u}{\partial^2 x} + \frac{\partial^2 u}{\partial^2 y} + \frac{\partial^2 u}{\partial^2 z}\right)$$

$$\frac{\partial(\rho uv)}{\partial x} + \frac{\partial(\rho v^2)}{\partial y} + \frac{\partial(\rho uw)}{\partial z} = -\frac{\partial(p_0)}{\partial y} + \rho\nu\left(\frac{\partial^2 v}{\partial^2 x} + \frac{\partial^2 v}{\partial^2 y} + \frac{\partial^2 v}{\partial^2 z}\right)$$

$$\frac{\partial(\rho uw)}{\partial x} + \frac{\partial(\rho uw)}{\partial y} + \frac{\partial(\rho w^2)}{\partial z} = -\frac{\partial(p_0)}{\partial z} + \rho\nu\left(\frac{\partial^2 w}{\partial^2 x} + \frac{\partial^2 w}{\partial^2 y} + \frac{\partial^2 w}{\partial^2 z}\right)$$

Conservation of Energy

$$\frac{\partial(\rho uT)}{\partial x} + \frac{\partial(\rho vT)}{\partial y} + \frac{\partial(\rho wT)}{\partial z} = \frac{\kappa}{\rho C_p}\left(\frac{\partial^2 T}{\partial^2 x} + \frac{\partial^2 T}{\partial^2 y} + \frac{\partial^2 T}{\partial^2 z}\right)$$

B. Geometry Creation and Mesh Generation

The setup was modelled for only entire fluid domain was used. It is logical to assume part of fluid domain instead of whole domain, that saves computation time. Domain has to build by considering inside fluid volume only.

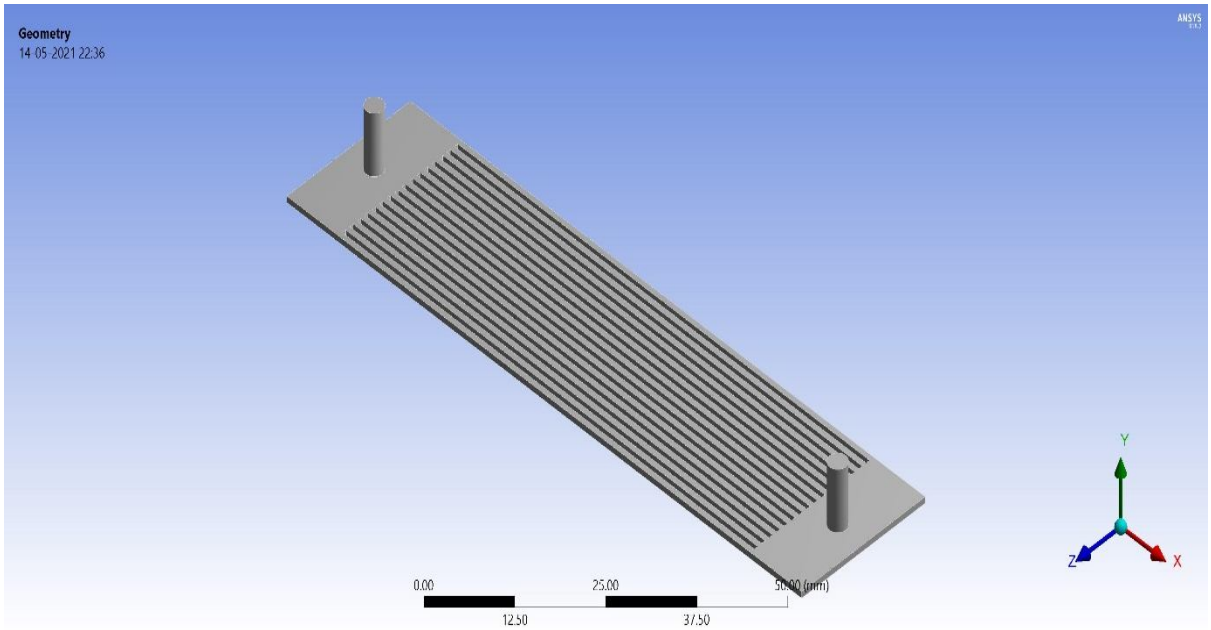

Fig. 12 Computational domain consider for analysis

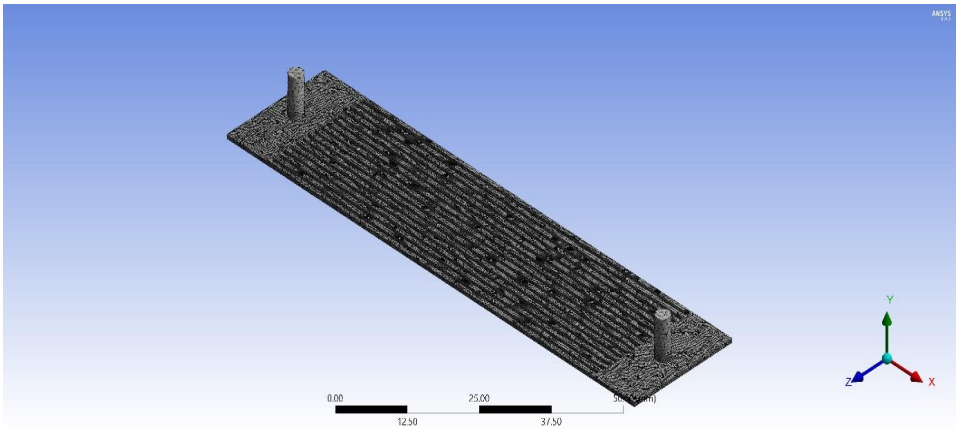

Fig. 13 Mesh Generation

Table II Mesh Matrices

Sr. No.	Parameter	Value
1	Nodes	140053
2	Elements	557949
3	Quality of element	0.82662
4	Skewness	0.24071
5	Aspect ratio	1.8863
6	Orthogonal quality	0.75802

C. Boundary Condition

All boundary conditions get implemented by the inclusion of additional source and/or sink terms in the finite volume formulation for computational cells at the boundaries.

Table III Boundary condition

Domain	Boundary condition	Parameters
Solid	Inlet	Mass flow rate
	Wall	Adiabatic
	Outlet	Pressure outlet

VI. NUMERICAL RESULT

This chapter are deals in CFD result and comparison between CFD and experimental result.

Table IV shows the Numerical result with respect to input boundary condition specified. Section A shows temperature contours at different input condition, section B shows the comparison between experimental and CFD result in fig. 16.

Table IV CFD Result

Sr. No	$\dot{m}_t$ (kg/s)	Q (W)	T_{in} (°C)	T_{out} (°C)	T_w (°C)	ΔP(Pa)
1	0.0006667	60	25	44.98	54.12	192.462
2	0.0006667	80	23	49.713	61.82	192.462
3	0.0006667	100	25	59.057	75.36	192.462
4	0.0005	60	25	49.849	58.11	138.736
5	0.0005	80	24	58.135	69.46	138.736
6	0.0005	100	24	68.197	83.21	138.736
7	0.0004167	60	26	55.241	62.62	104.453
8	0.0004167	80	25	64.286	73.96	104.453
9	0.0004167	100	26	78.579	92.05	104.453

A. Temperature Contours

Fig. 14 shows temperature contour of all cases. User define temperature range is selected for all cases to visualized temperature difference. The temperature range selected was inlet temperature of 23 °C to maximum outlet temperature of 78.579 °C.Fig. Shows the final temperature contours for mass flow rate of 0.0006667 kg/s, 0.0005 kg/s and 0.0004167 kg/s and heat input as 100W. Fig.14 (A) for mass flow rate of 0.0006667 kg/s and heat input as 100 W, Fig.14 (B) for mass flow rate of 0.0005 kg/s and heat input as 100 W and Fig. 14 (C) for mass flow rate of 0.0004167 kg/s and heat input as 100 W.

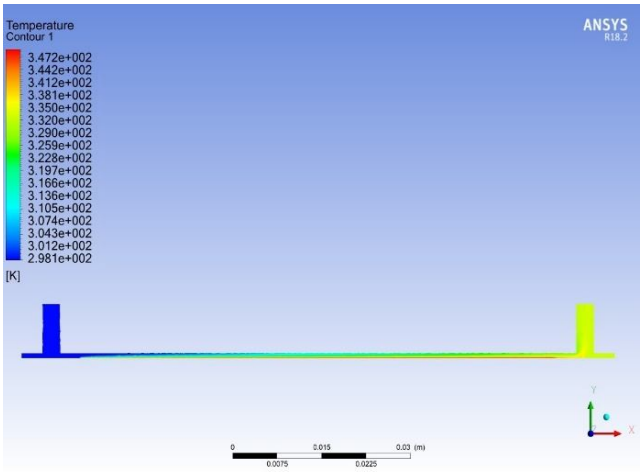

(A)

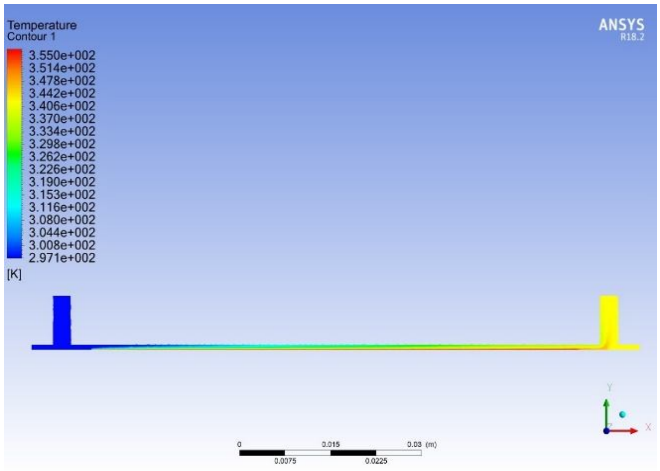

(B)

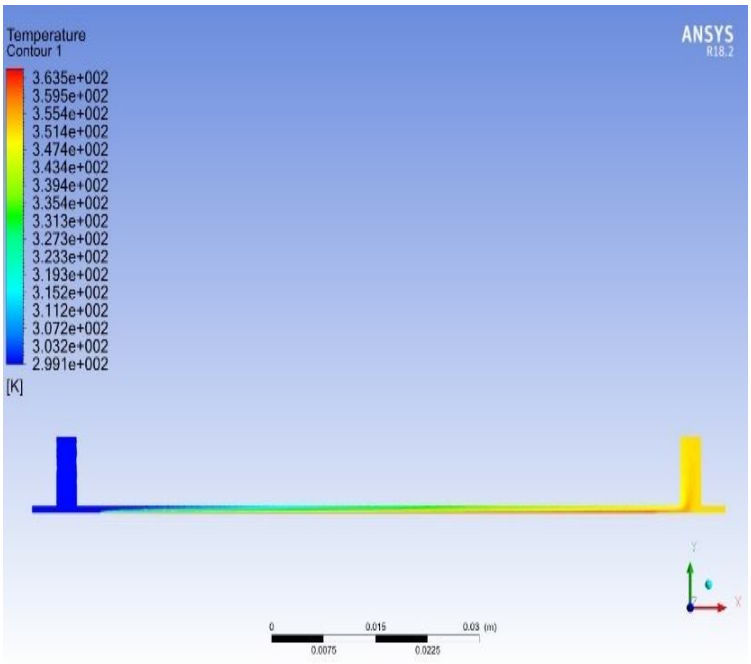

(C)

Fig. 14 Temperature contours at different mass flow rate as A) 0.0006667 kg/s B) 0.0005 kg/s and C) 0.0004167 kg/s at heat input 100W.

Fig. Shows the final temperature contours for mass flow rate of 0.0006667 kg/s, 0.0005 kg/s and 0.0004167 kg/s and heat input as 80W. Fig A for mass flow rate of 0.0006667 kg/s and heat input as 80 W, Fig B for mass flow rate of 0.0005 kg/s and heat input as 80 W and Fig C for mass flow rate of 0.0004167 kg/s and heat input as 80 W.

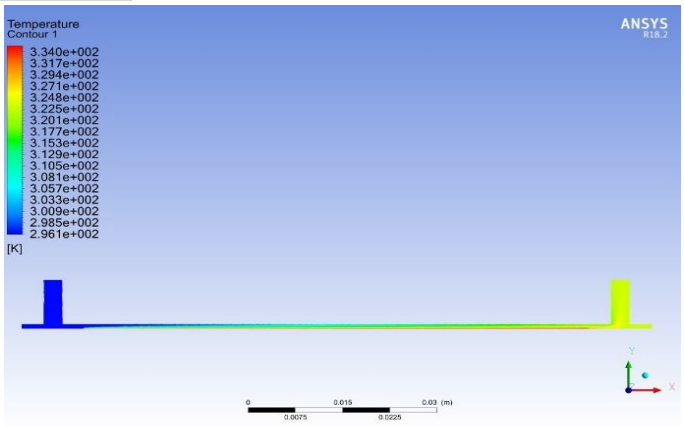

(A)

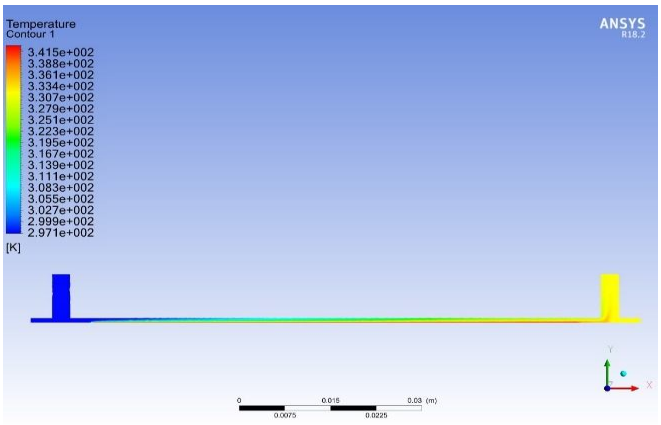

(B)

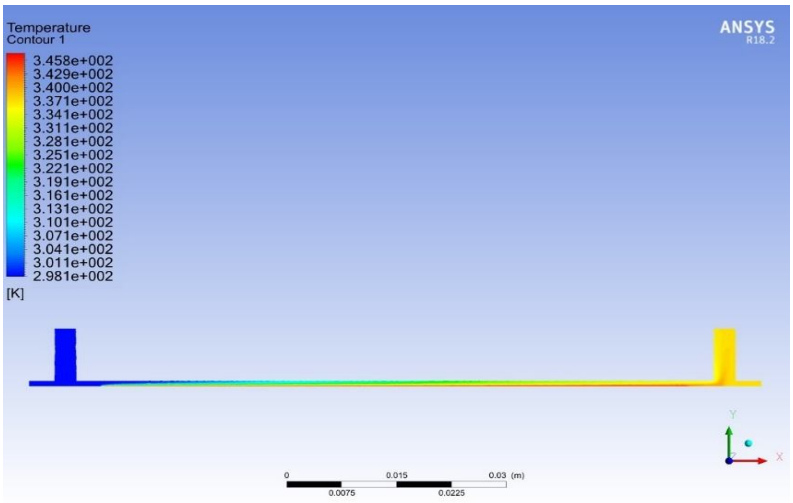

(C)

Fig. 15 Temperature contours at different mass flow rate as A) 0.0006667 kg/s B) 0.0005 kg/s and C) 0.0004167 kg/s at heat input 80W.

B. Comparison Between Numerical and Experimental Result

Fig. 16 shows experimental and numerical temperature difference with respect to heat flux. Maximum error between experimental and numerical is found to be 3.44% as shown in table V which shows matching of numerical and experimental result.

Table V Error between experimental and numerical result

Sr. No.	ΔT (°C)		
	Experimental	Numerical	Error (%)
1	20.66667	19.98	3.44
2	27.5	26.713	2.95
3	34.66667	34.057	1.79
4	25.16667	24.849	1.28
5	34.66667	34.135	1.56
6	44.66667	44.197	1.06
7	29.5	29.241	0.89
8	39.66667	39.286	0.97
9	52.16667	52.579	0.78

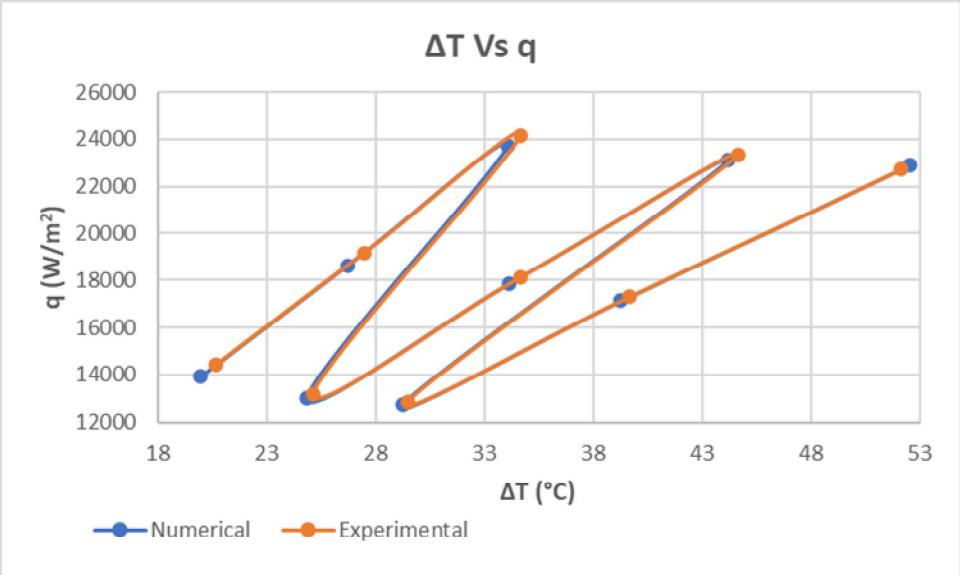

Fig. 16 Comparison between numerical and experimental results

VII. CONCLUSIONS

The advantages and limitation of hydrophobic microchannel was studied in present studied. Following are the conclusion drawn from experimental and numerical result:

1) Hydrophobic surface are more advantages than non-hydrophobic as its friction factor is less than theoretical friction factor.
2) In present study, Reynold number is directly proportion to the pressure drop whereas it is inversely proportional to the friction factor. This is because of flow nature of water.
3) Heat transfer coefficient is increases with increase in pressure drop of microchannel.
4) By keeping the mass flow rate high heat transfer is increases.
5) Maximum error between experimental numerical was found to be 3.44 % maximum.

A. Nomenclature

Q Heat transfer (W)
q Heat flux (W/m^2)
h Heat transfer coefficient (W/m^2-K)
k Thermal conductivity (W/m-K)
D_h Hydraulic diameter (m)
S Surface area (m^2)
T_{in} Inlet temperature (K)
T_{out} Outlet temperature (K)
ΔT Temperature difference (K)
T_w Wall temperature (K)
T_s Surface temperature (K)
T_f Fluid temperature (K)
m_t Total mass flow rate (kg/sec)
ΔP Pressure drop (Pa)
R_e Reynold number
C_p Specific heat capacity (J/Kg-K)
Q_w Heat removed by water (W)
F_{exp} Experimental frictional factor
F_{th} Theoretical frictional factor

REFERENCES

[1] Tuckerman D. B., and Pease R. F., High Performance Heat Sinking for VLSI, IEEE Electron. Device Letter, EDL-2 (1981) 126–129.
[2] S. Sasaki, and T. Kishimoto, optimal structure for microgrooved cooling fin for high-power LSI devices, Electronics and Mechanics technology laboratories 22 (1986).
[3] B. X. Wang, X. F. Peng, Experimental investigation on liquid forced convection heat transfer through microchannels, Int. Journal Heat Mass Transfer 37 (1994) 73-82.
[4] X. F. Peng, G. P. Peterson, Convective heat transfer and flow friction for water flow in microchannel structures, Int. Journal Heat Mass Transfer 39 (1996) 2599-2608.
[5] Y. Mukarami, B. Mikic, Parametric optimization of multichanneled heat sinks for VLSI chip cooling, IEEE transactions on components & packaging technologies 24 (2001) 2-9.
[6] S. G. Kandlikar, and W. J. Grande, Evolution of Microchannel Flow Passages - Thermohydraulic Performance and Fabrication Technology, Heat Transfer Engineering 24 (2003) 3-17.
[7] H. Y. Zhang, D. Pinjala, T. N. Wong, K. C. Toh, Y. K. Joshi, Single-phase liquid cooled microchannel heat sink for electronic packages, Applied Thermal Engineering 25 (2005) 1472–1487.
[8] P. S. Lee, S. V. Garimella, D. Liu, Investigation of heat transfer in rectangular microchannels, International Journal of Heat and Mass Transfer 48 (2005) 1688–1704.
[9] J. Jiang, Y. Hao, M. Shi, Fluid Flow and Heat Transfer Characteristics in Rectangular Microchannels, Heat Transfer-Asian Research, 37(4), 2008. 197-207.
[10] S. S. Heish, C. Y. Lin, Convective heat transfer in liquid microchannels with hydrophobic and hydrophilic surfaces, Int. Journal of Heat & Mass Transfer 52 (2009) 260-270.
[11] Y. Cheng, J. Xu, Y. Sui, Numerical study on drag reduction and heat transfer enhancement in microchannels with superhydrophobic surfaces for electronic cooling, Applied Thermal Engineering (2014) 1-11.
[12] J. Zhou, Z. Yan, Q. Gao, Development and Application of Micro Channel Heat Exchanger for Heat Pump, 12th IEA Heat Pump Conference (2017) P.3.1.5.
[13] A. Heidarian, R. Rafee, M. S. Valipour, Effects of wall hydrophobicity on the thermohydraulic performance of the microchannels with nanofluids, Int. Communication in Heat and Mass Transfer 117 (2020) 104758.
[14] M. Spizzichino, G. Sinibaldi, G.P. Romano, Experimental investigation on fluid mechanics of micro-channel heat transfer devices, Experimental Thermal and Fluid Science 118 (2020) 110141.

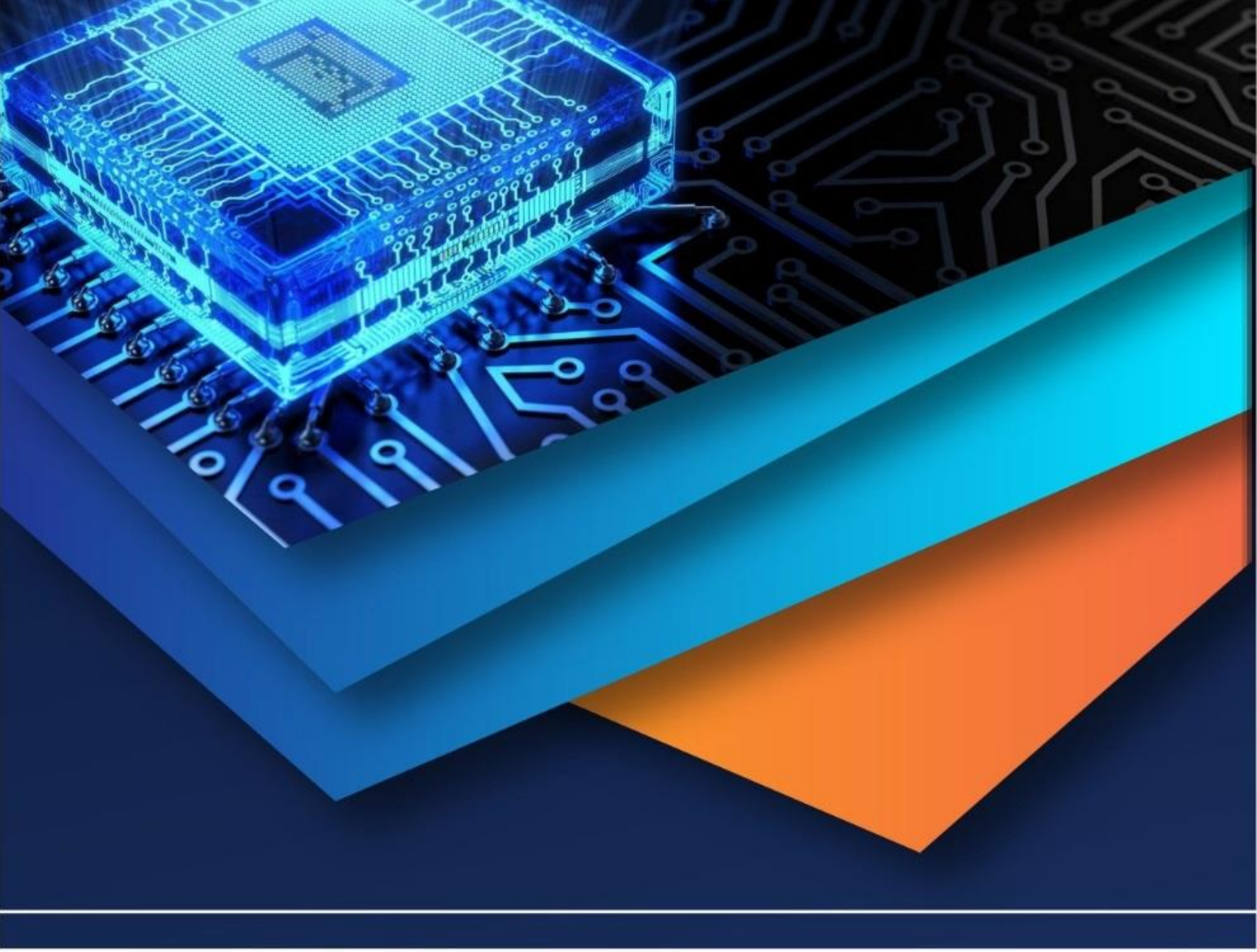

10.22214/IJRASET

45.98

IMPACT FACTOR: 7.129

IMPACT FACTOR: 7.429

INTERNATIONAL JOURNAL FOR RESEARCH

IN APPLIED SCIENCE & ENGINEERING TECHNOLOGY